In vivo identification of genes that modify ether-a-go-go-related gene activity in *Caenorhabditis elegans* may also affect human cardiac arrhythmia

Christina I. Petersen*, Toni R. McFarland*, Svetlana Z. Stepanovic*, Ping Yang†, David J. Reiner‡, Kenshi Hayashi*, Alfred L. George§, Dan M. Roden†, James H. Thomas¶, and Jeffrey R. Balser*‖

*Department of Anesthesiology and Divisions of †Clinical Pharmacology and §Genetic Medicine, Vanderbilt University, Nashville, TN 37232

Edited by Barbara J. Meyer, University of California, Berkeley, CA, and approved June 10, 2004 (received for review October 1, 2003)

Human ether-a-go-go-related gene (HERG) encodes the pore-forming subunit of I_{Kr}, a cardiac K^+ channel. Although many commonly used drugs block I_{Kr}, in certain individuals, this action evokes a paradoxical life-threatening cardiac rhythm disturbance, known as the acquired long QT syndrome (aLQTS). Although aLQTS has become the leading cause of drug withdrawal by the U.S. Food and Drug Administration, DNA sequencing in aLQTS patients has revealed HERG mutations only in rare cases, suggesting that unknown HERG modulators are often responsible. By using the worm *Caenorhabditis elegans*, we have developed *in vivo* behavioral assays that identify candidate modulators of *unc-103*, the worm HERG orthologue. By using RNA-interference methods, we have shown that worm homologues of two HERG-interacting proteins, Hyperkinetic and K channel regulator 1 (KCR1), modify *unc-103* function. Examination of the human KCR1 sequence in patients with drug-induced cardiac repolarization defects revealed a sequence variation (the substitution of isoleucine 447 by valine, I447V) that occurs at a reduced frequency (1.1%) relative to a matched control population (7.0%), suggesting that I447V may be an allele for reduced aLQTS susceptibility. This clinical result is supported by *in vitro* studies of HERG dofetilide sensitivity by using coexpression of HERG with wild-type and I447V KCR1 cDNAs. Our studies demonstrate the feasibility of using *C. elegans* to assay and potentially identify aLQTS candidate genes.

Caenorhabditis elegans unc-103 shares 70% amino acid identity with HERG in the conserved transmembrane and pore regions of the protein (see Scheme 1).

Scheme 1.

Studies using *unc-103* promoter GFP reporter constructs reveal expression of *unc-103* in body-wall muscle, egg-laying muscles, pharyngeal muscles, and neurons that innervate these tissues (D.J.R, J.H.T., and R. Garcia, unpublished data). Worm strains carrying mutations in this gene, *unc-103* (*n500*) and *unc-103* (*e1597*), were isolated in screens for locomotion-defective mutants (1). Analysis of both of these neomorphic mutant strains revealed the same mutation: conversion of a conserved alanine in the S6 transmembrane domain to a threonine (A334T, indicated in bold above). Our studies reveal that these mutant worms exhibit profound neuromuscular defects, and the severity of these defects is sensitive to modulators that decrease the level of mutant channel activity. Further, the human homologues of these modulators may have physiologically relevant interactions with human ether-a-go-go-related gene (HERG) and represent acquired long QT syndrome (aLQTS) candidate genes.

Methods

Molecular Biology. The human K channel regulator 1 (KCR1) cDNA, an IMAGE clone (no. 650823) was purchased from Research Genetics (Huntsville, AL). Site-directed mutagenesis was performed as described (2). For *in vitro* cRNA transcription, we used the SP6 mMessage mMachine high-yield capped RNA transcription kit (Ambion, Austin, TX). For RNA interference (RNAi) vectors, we PCR-amplified fragments of 0.9–1.5 kb of the target gene from *C. elegans* genomic DNA. The PCR oligonucleotides were designed to ensure no more than 60% nucleotide identity to any other sequence in the *C. elegans* genome. PCR products were ligated into pGEM-TEZ vector, cut with *Not*I, and ligated into the L4440 vector (A. Fire laboratory database, available at ftp://ftp.wormbase.org/pub/elegans_vector) containing isopropyl β-D-thiogalactoside-inducible T7 promoters on both sides of the coding sequence. The clones were transformed into double-stranded RNase-deficient bacteria [HT115 (DE3)].

***C. elegans* Behavioral Assays.** All strains were obtained from the *Caenorhabditis* Genetics Center (St. Paul). Locomotion-assay protocols were as follows. Young adult hermaphrodites were picked to individual wells of a 96-well plate containing liquid M9. Side-to-side thrashing movements of the head were counted for 1 min. For pharyngeal-pumping assays, young adult hermaphrodites were placed onto a seeded plate and their pharyngeal pumping was observed for 1 min with a dissecting scope. By using custom-designed software (J.H.T.), a computer key was pressed and held during each observed pause. Upon resumption of pumping, the key was released. At the end of the assay, the cumulative pause time, number of pauses, and mean pause length were calculated for each worm. For all assays, we tested 10 worms per condition on 3 different days (for a total of 30 worms), and we reported the results as mean ± SEM, with significance defined at $P < 0.05$ (pairwise comparisons, Student's *t* test). For drug assays, young adult hermaphrodites were rinsed from food plates, washed three times in H_2O, exposed to drug in 1.0–1.2 ml of H_2O, and incubated for 1 h at room temperature (22–24°C) with gentle rocking. The worms were placed on drug-containing plates and assayed. For RNAi assays,

This paper was submitted directly (Track II) to the PNAS office.

Abbreviations: HERG, human ether-a-go-go related gene; aLQTS, acquired long QT syndrome; KCR1, K channel regulator 1; RNAi, RNA interference; cKCR1, *Caenorhabditis elegans* KCR1; *lf*, loss-of-function.

‡Present address: Department of Human Genetics, 106 West Poplar Street, Carrboro, NC 27510.

¶Present address: Department of Genome Sciences, University of Washington, Seattle, WA 98195.

‖To whom correspondence should be addressed at: Department of Anesthesiology, 504 Oxford House, 1313 21st Avenue South, Nashville, TN 37232-4125. E-mail: jeff.balser@vanderbilt.edu.

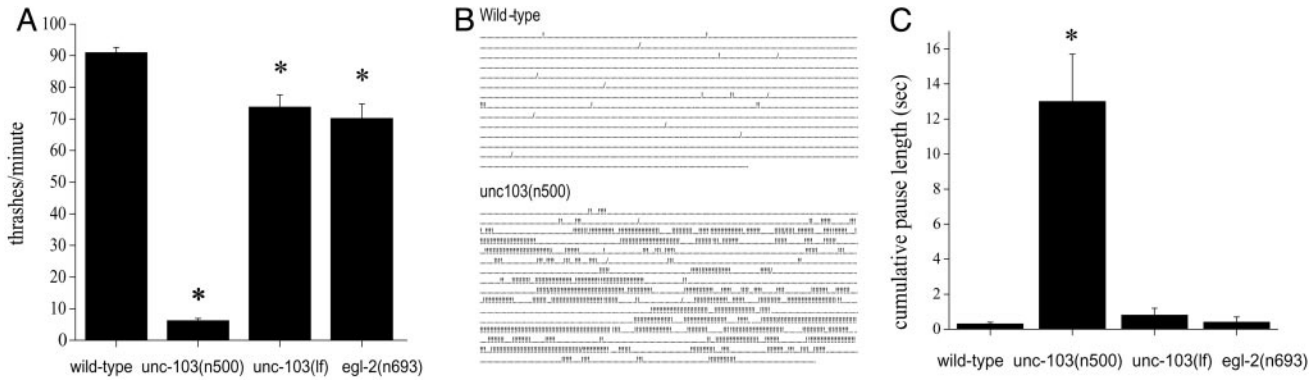

Fig. 1. Characterization of *unc-103* (*n500*) behavioral defects. (*A*) Locomotion measured by liquid thrashing assays for wild-type, *unc-103* (*n500*), *unc-103* (*lf*), and *egl-2* (*n693*) worms. Wild-type worms thrashed at a rate of 91.0 ± 1.6 thrashes per min vs. 6.2 ± 0.8 thrashes per min for *unc-103* (*n500*). *unc-103* (*lf*) and *egl-2* (*n693*) also thrashed at reduced rates, compared with wild type (73.8 ± 3.8 and 70.2 ± 4.6, respectively; $n = 30$ worms for each strain). (*B*) Representative ethogram of the pharyngeal pumping pattern for wild-type and *unc-103* (*n500*) worms. Each symbol represents a 0.2-sec ''snapshot'' from a continuous 60-sec observation period (see *Methods*). Exclamation points represent pauses, periods represent normal pumping, and slash marks separate distinct 60-sec assays from a single worm. For illustrative purposes, we displayed 10 ethogram recordings strung together from 10 (of the 30) worms. (*C*) Cumulative time spent in a pumping pause during each a 60-sec assay, measured for each strain from *A*. *unc-103* (*n500*) and wild type differed (13.0 ± 2.7 and 0.3 ± 0.1 sec, respectively). *unc-103* (*lf*) and *egl-2* (*n693*) were indistinguishable from wild type (0.8 ± 0.4 and 0.4 ± 0.3, respectively; $n = 30$ worms for each strain).

control and experimental bacteria were plated on nematode growth medium plates containing 1 mM isopropyl β-D-thiogalactoside. L1 worms were placed on the plates and observed for behavioral effects 48 h later. Both pBluescript- and GFP-L4440-transformed HT115 (DE3) control bacteria were used and gave similar results.

Oocyte Harvest from *Xenopus laevis*. Oocytes were isolated from adult *X. laevis* and digested with 2 mg/ml type 1A collagenase (Sigma) in calcium-free ND96 solution containing 96 mM NaCl, 2 mM KCl, 5 mM $MgCl_2$, and 5 mM Hepes (pH 7.6). Oocytes were stored in ND96 with 0.6 mM $CaCl_2$/50 μg/ml tetracycline/100 μg/ml streptomycin/550 μg/ml sodium pyruvate. Stage V and VI oocytes were injected with 3–10 ng of cRNA (Picospritzer II, General Valve, Cleveland) and incubated at room temperature for 12–24 h and then at 15°C.

Electrophysiological Recordings. Oocyte currents were recorded at 22–24°C in ND96 by using a two-microelectrode voltage clamp 2–5 days after cRNA injection. Electrodes of 0.4–2.0 MΩ were filled with 3 M KCl. An OC-725C (Warner Instruments, Hamden, CT) oocyte clamp, PCLAMP 8.1 software, and a Digidata 1322A analog-to-digital (A/D) board (Axon Instruments, Union City, CA) were used to send voltage commands and collect data. The voltage dependence of activation was determined by fitting a Boltzmann function, $y = [1 + \exp(V - V_{1/2}/k_B)]^{-1}$ to the data.

Dofetilide blockage of I_{Kr} was assayed by whole-cell patch clamp (Axopatch 200B, Digidata 1200) of Chinese hamster ovary K1 cells, 2 days after HERG transfection. The intracellular solution was 110 mM KCl/5 mM K_2ATP/5 mM K_4BAPTA/1 mM $MgCl_2$/10 mM Hepes (pH 7.2). The external solution was 140 mM NaCl/5.4 mM KCl/2 mM $CaCl_2$/1 mM $MgCl_2$/10 Hepes/10 glucose (pH 7.4), with pipette resistances of 2–5 MΩ. Cell and pipette capacitances were nulled, and series resistance was compensated by 80%. HERG, HERG plus KCR1, and HERG plus I447V KCR1 data were acquired (PCLAMP 8.0) and compared by using a 3 × 4 (condition × concentration) univariate ANOVA (SPSS, Chicago). Post hoc analysis of observed means was corrected for multiple comparisons by using the Bonferroni criterion.

Screening for Allelic Variants. Single-stranded conformational polymorphism (SSCP) analysis was used to identify polymorphisms in the coding region of the KCR1 gene. The amplification reactions were carried out in 50-μl volumes comprising 0.4 μM of each primer (forward, 5′-TTTCAAAGATATGCAATTCTG-3′; and reverse, 5′-AAGTCCATTTTTACAGTTCA-3′), 1× PCR buffer, and 200 μM dNTPs. PCRs were performed at 95°C for 10 min, 95°C for 30 sec, 54°C for 30 sec, and 72°C for 30 sec for 30 cycles, and then at 72°C for an additional 10 min. SSCP analysis was performed on 0.5× mutation-detection enhancement gels electrophoresed overnight at 6 W and stained with silver nitrate. Abnormal conformers were excised from the gel, eluted into sterile water, reamplified, and sequenced.

Results

***unc-103* (*n500*) Behavioral Defects.** By using behavioral assays that assess neuromuscular function, worms homozygous for the *unc-103* (*n500*) mutation were compared with wild-type as well as two control strains. The controls included a loss-of-function (*lf*) mutant, *unc-103* (*e1597n1213*), which was predicted to be a genetic null for the protein based on nucleotide sequence obtained from the mutant strain (D.J.R. and J.H.T., unpublished data), and *egl-2* (*n693*), the K^+ channel with the closest amino acid identity to *unc-103* (3). *egl-2* (*n693*) also carries an alanine-to-valine mutation in the S6 position analogous to *unc-103* (*n500*). Fig. 1*A* shows the result of liquid-thrashing assays used to measure the locomotion ability of *unc-103* (*n500*) worms. *unc-103* (*n500*) worms thrash at a 15-fold lower rate than wild type, whereas *egl-2* (*n693*) and *unc-103* (*lf*) worms exhibit only a small reduction, compared with wild type.

unc-103 (*n500*) worms also display a marked pharyngeal-pumping defect (see Figs. 6 and 7 and Movies 1 and 2, which are published as supporting information on the PNAS web site). Fig. 1*B* shows an ''ethogram'' of wild-type and *unc-103* (*n500*) pumping patterns. Data recorded from 10 consecutive assays in both wild type and *unc-103* (*n500*) are shown. In wild type, the pharynx contracts in a rhythmic manner (periods, Fig. 1*B*) and rarely pauses (exclamation points, Fig. 1*B*), whereas the *unc-103* (*n500*) cumulative pause length is 40 times longer than the wild type (summarized data, Fig. 1*C*). Fig. 1*C* shows that, in contrast to *unc-103* (*n500*), *unc-103* (*lf*) and *egl-2* (*n693*) worms do not display pharyngeal-pumping pauses.

Effects of HERG-Blocking Drugs on the *unc-103* (*n500*) Phenotype. As an initial strategy, we examined whether HERG-blocking compounds rescue *unc-103* (*n500*) behavioral phenotypes. No rescue was observed with high (100 μM) concentrations of dofetilide,

Table 1. Effects of 100 μM D-sotalol on wild-type and mutant worms

Assay	Condition	Genotype: Wild type	*unc-103* (*n500*)	*unc-103* (*lf*)	*egl-2* (*n693*)
Locomotion	Control	85.2 ± 4.4	8.4 ± 1.4	59.4 ± 5.2	69.6 ± 5.0
Thrashes per worm per min	D-sotalol	94.2 ± 4.8	21.4 ± 2.6*	58.4 ± 5.6	73.6 ± 4.0
Pumping	Control	0.0 ± 0.0	2.2 ± 0.4	0.1 ± 0.0	0.6 ± 0.1
Mean pause length, sec	D-sotalol	0.1 ± 0.0	2.9 ± 0.7	0.1 ± 0.0	0.3 ± 0.1

*$P < 0.05$.

E-4031, and quinidine (data not shown). However, 100 μM D-sotalol partially rescued the thrashing defect in *unc-103* (*n500*) without affecting the *egl-2* (*n693*) and *unc-103* (*lf*) thrashing rates (Table 1). D-sotalol did not effect pharyngeal pumping in *unc-103* (*n500*) worms and did not alter either phenotype in wild-type worms, suggesting that the locomotion defect is either more sensitive to the effects of reduction in UNC-103 (*n500*) activity and/or that the mutant channel resides in a tissue locus that is more sensitive to D-sotalol blockage. Concentrations of D-sotalol up to 1 mM did not further increase the thrashing rate of *unc-103* (*n500*) (data not shown).

***unc-103* RNAi.** The modest effect of HERG blockers on *unc-103* (*n500*) was not surprising because species differences in the S6 domain reside in putative methanesulfonanalide drug binding sites (4). As an alternative strategy for detecting physiological effects of candidate *unc-103*-modifying gene products, we used RNAi (5) to knock-down message. To test this approach, worms that were fed bacteria containing an inducible transcription vector of a portion of the *unc-103* nucleotide sequence or control bacteria were observed for rescue of locomotion and pharyngeal-pumping defects. Fig. 2*A* shows that locomotion was partially restored in *unc-103* RNAi-treated *unc-103* (*n500*) worms, whereas there was no effect on wild-type or either control strain. *Unc-103* RNAi also partially rescues the pharyngeal-pumping defect of *unc-103* (*n500*) (Fig. 2*B*), whereas again, *unc-103* RNAi had no effect on wild-type, *unc-103* (*lf*), or *egl-2* (*n693*) pharyngeal pumping. These data demonstrate that manipulations that result in reduction of mutant channel activity in *unc-103* (*n500*) worms result in a gene-specific and quantifiable partial rescue of both mutant phenotypes. It is noteworthy that *unc-103* RNAi had no effect on wild-type worms, suggesting RNAi does not reduce UNC-103 channel number to the functional level of *unc-103* (*lf*) (Fig. 2*A*). This result implies that phenotypes associated with the *unc-103* (*n500*) strain are more sensitive (than wild type) to interventions that reduce channel number.

HERG A653T Electrophysiology. Efforts to express *unc-103* or *unc-103* (*n500*) clones in heterologous-expression systems proved to be unsuccessful and may require an unidentified accessory subunit for proper trafficking or function. To gain preliminary insights into biophysical mechanisms that may underlie the behavioral phenotypes displayed by *unc-103* (*n500*), we constructed the analogous alanine to threonine mutation in HERG (A653T) and expressed this clone in *Xenopus* oocytes. Representative wild-type and A653T currents are shown (Fig. 3*A*) in response to incremental depolarizing membrane potentials (clamp protocol, Fig. 3*A Top*). Although both channels generate outward K^+ current, the mutant displays abnormal gating behavior. The current–voltage relationship (Fig. 3*B*), measured at the indicated position (arrows, Fig. 3*A*), displays a 22-mV hyperpolarizing shift in half-activation potential ($V_{1/2}$) (Fig. 3*B*, dotted line). If the mutant *C. elegans* channel displayed an analogous voltage shift to A653T, UNC-103 (*n500*) would conduct greater outward current at negative potentials (hyperpolarizing the cell) than the wild-type channel. Such hyperpolarization is consistent with the reduced-excitability phenotypes observed for *unc-103* (*n500*) (pharyngeal pauses and flaccid paralysis). Indeed, *Xenopus* oocytes injected with HERG A653T have resting-membrane potentials that are 17 mV more hyperpolarized than oocytes injected with wild-type HERG (Fig. 3*C*).

***C. elegans KCR1* (*cKCR1*) and *mec-14* RNAi.** Because our goal was to identify physiologically relevant ERG-modifying proteins, we assayed for rescue of the *unc-103* (*n500*) phenotypes by exposing mutant worms to RNAi constructs for candidate K^+ channel-modifying proteins. We assayed four different *C. elegans* genes in this regard, basing our selections on sequence similarity to proteins previously demonstrated to modify, K^+ channel func-

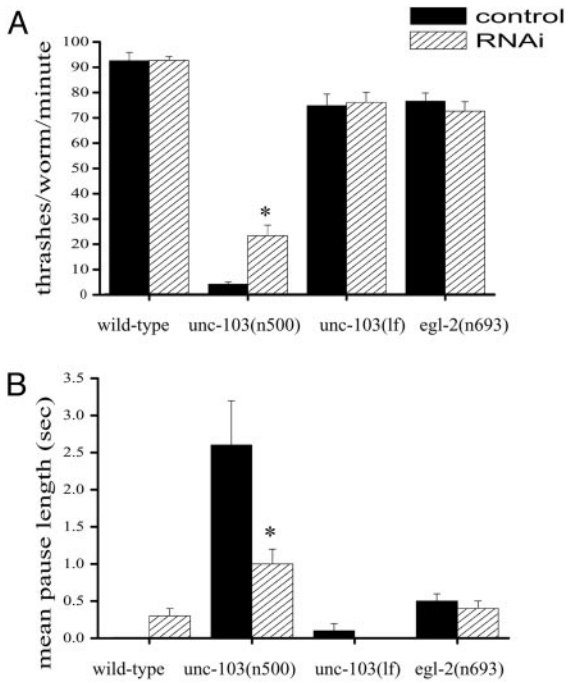

Fig. 2. RNAi partially rescues the *unc-103* (*n500*) defects. The worm strains used in Fig. 1 were fed bacteria containing *unc-103* DNA or a control (see *Methods*). (*A*) Locomotion was assayed as shown in Fig. 1*A*. *unc-103* RNAi increased the thrashing rate for *unc-103* (*n500*) from 4.2 ± 0.8 to 23.4 ± 4.2 thrashes per worm per min ($n = 30$ worms each). *unc-103* RNAi had no effect on wild-type, *unc-103* (*lf*), and *egl-2* (*n693*) thrashing rates (92.6 ± 3.2 and 92.8 ± 3.2 for wild type; 74.8 ± 4.6 and 76.2 ± 3.8 for *unc-103* (*lf*); and 76.6 ± 3.2 and 72.6 ± 3.8 for *egl-2* (*n693*); rates are given for control and *unc-103* RNAi-treated worms, respectively; $n = 30$ for each condition). (*B*) Pharyngeal pumping assayed as shown in Fig. 1*C*, but data are presented as mean pause length. *unc-103* RNAi decreased pause length from 2.6 ± 0.6 to 1.0 ± 0.2 sec in *unc-103* (*n500*) ($n = 30$ worms each) but had no effect on wild-type, *unc-103* (*lf*), or *egl-2* (*n693*) (0 and 0.3 ± 0.1 for wild-type; 0.1 ± 0.1 and 0 for *unc-103* (*lf*); and 0.5 ± 0.1 and 0.4 ± 0.1 for *egl-2* (*n693*), control, and *unc-103* RNAi, respectively; $n = 30$ worms for each condition). *, Comparison of RNAi with control within the same strain.

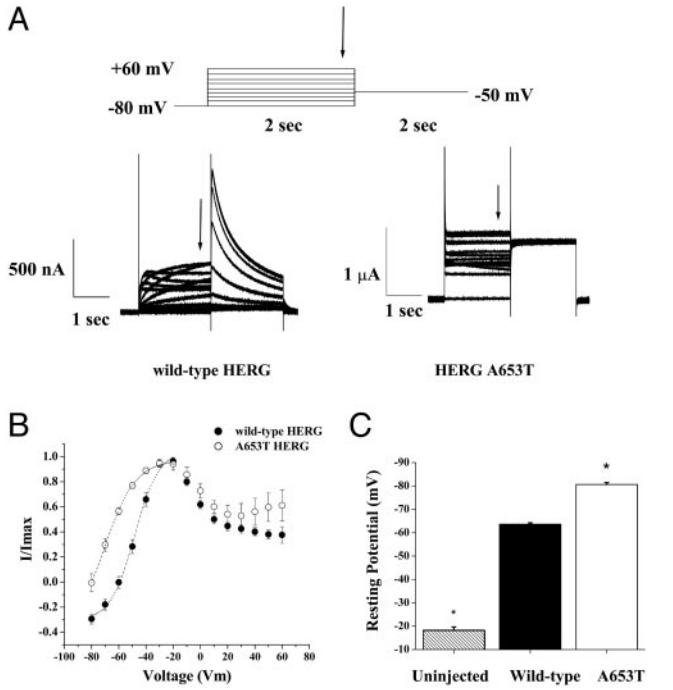

Fig. 3. Electrophysiological analysis of A653T. (*A*) Current traces from wild-type and A653T HERG in *Xenopus* ooctyes. The voltage-clamp protocol is shown (*Top*). (*B*) Current was measured at the time indicated by the arrows in *A* and plotted against membrane potential. The rising phase of the current–voltage relationship for each cell was fitted by a Boltzmann equation (see *Methods*). $V_{1/2}$ was -48.3 ± 1.3 ($n = 10$) and -70.9 ± 2.6 mV ($n = 5$) in wild type and A653T, respectively. (*C*) The resting-membrane potential was measured in *Xenopus* oocytes injected with wild-type HERG ($n = 99$), A653T ($n = 74$), or uninjected oocytes ($n = 76$). Resting potentials were as follows: -18.0 ± 1.4, -63.6 ± 0.6, and -80.6 ± 0.8 mV for uninjected, wild-type, and A653T respectively. *, $P < 0.05$ vs. wild type.

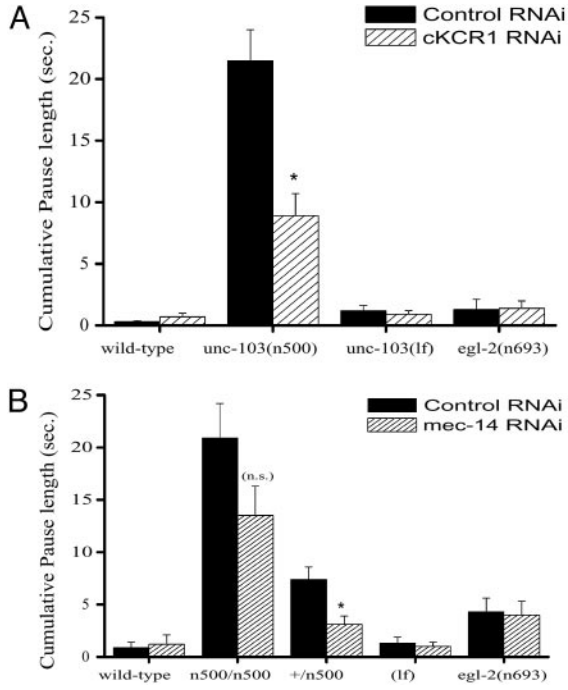

Fig. 4. *In vivo* analysis of *cKCR1* and *mec-14* effects on *unc-103* (*n500*). (*A*) The four worm strains assayed as shown in Fig. 1 were exposed to *cKCR1* RNAi (see *Methods*) and assayed for pharyngeal-pumping defects, as described in Fig. 1. The cumulative pause length in *unc-103* (*n500*) worms was decreased by 12 sec in cKCR1 RNAi-exposed worms compared with control treated worms (21.5 ± 2.5 and 8.9 ± 1.8 in control and RNAi-treated worms, respectively; $n = 30$ worms each). *cKCR1* RNAi had no effect on wild-type, *unc-103* (*lf*), and *egl-2* (*n693*) worms (0.3 ± 0.1 and 0.7 ± 0.3 for wild-type, 1.2 ± 0.4 and 0.9 ± 0.3 in *unc-103* (*lf*), and 1.3 ± 0.8 and 1.4 ± 0.6 in *egl-2* (*n693*), for control and cKCR1 RNAi-treated worms, respectively ($n = 30$ worms for each condition). (*B*) In addition to the four worm strains assayed as shown in Fig. 1, we also assayed wild-type/(*n500*) (+/*n500*) heterozygote worms. Worms were exposed to *mec-14* RNAi and assayed for pharyngeal-pumping defects. The cumulative pause length in +/*n500* worms was decreased by >50% in *mec-14* exposed worms compared with control treated worms (7.4 ± 1.2 and 3.1 ± 0.8 in control and RNAi-treated worms, respectively; $P < 0.05$, $n = 70$ worms for both conditions). *mec-14* also reduced the pause length in *unc-103* (*n500*) worms, although not significantly (20.9 ± 3.3 and 13.5 ± 2.8 for control and *mec-14* RNAi-treated worms, respectively; $n = 30$ worms for both conditions). *mec-14* RNAi had no effect on wild-type, *unc-103* (*lf*), and *egl-2* (*n693*) worms [0.9 ± 0.5 and 1.2 ± 0.9 for wild-type, 1.3 ± 0.6 and 1.0 ± 0.4 in *unc-103* (*lf*), and 4.3 ± 1.3 and 4.0 ± 1.3 in *egl-2* (*n693*); results are given for control and *mec-14* RNAi-treated worms, respectively; $n = 30$ worms for each condition).

tion in heterologous-expression systems. C29F5.4 shows the greatest amino acid identity (18%) to MiRP1, a protein that has been shown to interact with HERG *in vitro* (6). C07D8.6 is one of a number of *C. elegans* proteins displaying similarity to Kvβ subunits and oxidoreductase enzymes. A family of these proteins is present in mammals, and they modify K^+ channel currents in heterologous-expression systems (for reviews, see refs. 7 and 8). T24D1.4 is the closest worm homologue to KCR1, a protein shown to interact with rat ether-a-go-go (EAG) (9) and HERG (10). F37C12.12 (*mec-14*) has the closest amino acid similarity to Hyperkinetic, a *Drosophila* protein shown to modify both EAG and HERG gating in *Xenopus* oocytes (11).

Although RNAi against C29F5.4 and C07D8.6 did not rescue *unc-103* (*n500*) phenotypes (locomotion or pharyngeal pumping), we did observe significant rescue with RNAi directed against *cKCR1* and *mec-14* (Fig. 4). Fig. 4*A* shows that the pharyngeal-pumping defect displayed a 42% decrease in the cumulative pause length after cKCR1 RNAi treatment, compared with *unc-103* (*n500*) worms treated with control bacteria. *cKCR1* RNAi had no effect on pumping in *unc-103* (*lf*) and *egl-2* (*n693*) (Fig. 4*A*) or on locomotion defects (data not shown) in *unc-103* (*n500*).

mec-14 is implicated in mechanotransduction and is proposed to regulate *C. elegans* epithelial Na^+ channel activity (12). RNAi to *mec-14* in *unc-103* (*n500*) worms did not result in significant improvement of pharyngeal pumping (Fig. 4*B*). Recognizing that the *unc-103* (*n500*) phenotype is particularly sensitive to channel number (Fig. 2), we genetically manipulated the number of *unc-103* (*n500*) channels by constructing wild-type/(*n500*) heterozygous (+/*n500*) worms (Fig. 4*B*). These worms presumably have less *unc-103* (*n500*) channel activity than homozygous *n500* mutants. Fig. 4*B* indicates that although pause length for the heterozygote is greater than it is for wild type, it is reduced substantially compared with the *n500* homozygote.

The effect of *mec-14* RNAi in +/*n500* heterozygote worms was pronounced. The cumulative pharyngeal-pumping pause length was decreased by >50%. The effects of RNAi to *mec-14* were specific because there was no pumping effect in wild-type, *unc-103* (*lf*), and *egl-2* (*n693*) worms treated with *mec-14* RNAi (Fig. 4*B*) and no effect on locomotion in the *unc-103* (*n500*) worms (data not shown). These findings not only reveal *in vivo* modification of *unc-103* (*n500*) activity by *mec-14*, but they also demonstrate the usefulness of heterozygote strains for raising the sensitivity of assays for *in vivo* interactions. The selective effect of *mec-14* or *cKCR1* RNAi treatment on pharyngeal pumping, relative to locomotion, also underscores the importance of using multiple behavioral assays to assess UNC-103 function because particular UNC-103–subunit interactions may

occur in only a subset of tissues. Also, the tissue(s) responsible for the pharyngeal-pumping defect of *unc-103* (*n500*) may be more amenable to RNAi effects than the tissue(s) responsible for the locomotion defects of *unc-103* (*n500*).

We assayed for synergistic effects between *cKCR1* or *mec-14* RNAi treatment and D-sotalol treatment in improving the pharyngeal pumping or locomotion defect of *unc-103* (*n500*) worms. We found no effect on either behavior from either *cKCR1* or *mec-14* RNAi treatment in D-sotalol-treated *unc-103* (*n500*) worms (data not shown).

KCR1 I447V Polymorphism. On the basis of our *in vivo* findings in *C. elegans*, we have undertaken genetic screens for mutations in human orthologues of *unc-103*-modifying proteins. Patients who previously exhibited severe repolarization abnormalities when exposed to HERG-blocking drugs (aLQTS patients) were compared with ethnicity-matched control patients. We sequenced the human KCR1 coding region in 92 aLQTS subjects, and we found an A-to-G transition at position 1339 that results in the substitution of isoleucine 447 by valine (I447V). Only two heterozygotes of 92 aLQTS patients have been identified [allele frequency of 2/184, 1.1%, vs. a 7% (10/142) allele frequency in the control population ($P < 0.05$; χ^2)]. hKCR1 I447V may, therefore, be a protective allele in patients exposed to QT-prolonging agents.

To test this hypothesis *in vitro*, we engineered the I447V polymorphism into the human KCR1 cDNA (I447V). We expressed both KCR1 and I447V with HERG in Chinese hamster ovary cells and assayed HERG current in the presence of the I_{Kr} blocker dofetilide by using the whole-cell patch-clamp technique. HERG-expressing cells were exposed to depolarizing pulses in the presence of external dofetilide. Fig. 5*A* shows representative tail currents recorded before (Pre-drug) and after drug exposure. The peak tail currents were fitted by a single exponential function (dotted line, Fig. 5*A*) to quantify the rate of development of drug blockage of HERG current (τ). Drug blockage was assayed for HERG, HERG plus KCR1, and HERG plus I447V KCR1, and the findings are plotted in Fig. 5*B*. The rate of dofetilide drug blockage of HERG was decreased significantly in the presence of wild-type KCR1 and more so with I447V KCR1, compared with HERG alone. By using the steady-state values of dofetilide blockage, we determined that the IC_{50} values for dofetilide blockage are as follows: 26.9 ± 13.1 nM, 33.6 ± 7.4 nM, and 44.7 ± 11.7 nM for HERG, HERG plus wild-type KCR1, and HERG plus I447V KCR1, respectively. These results are consistent with KCR1 I447V exerting a greater protective effect, relative to wild-type KCR1, against drug blockage of I_{Kr}.

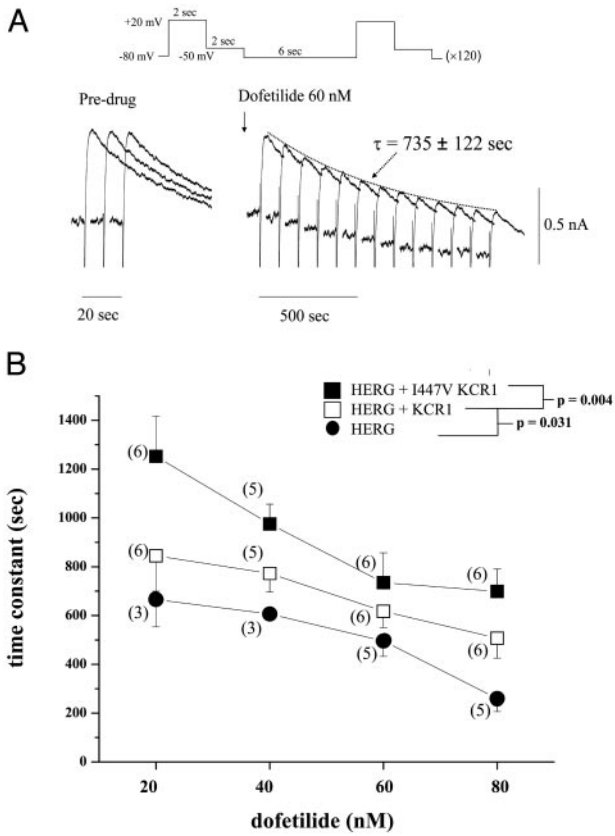

Fig. 5. Effects of KCR1 and I447V on dofetilide blockage of HERG current. HERG cDNA was coexpressed with either KCR1 or I447V KCR1 in Chinese hamster ovary cells, and current was measured in the presence of varying concentrations of dofetilide (20–80 nM) by using a whole-cell voltage clamp. (*A*) HERG-expressing Chinese hamster ovary cells were depolarized to +20 mV, and peak tail currents were measured upon hyperpolarization to −50 mV in the presence of external dofetilide. This protocol was repeated 120 times (0.1 Hz) for each cell (see voltage protocol above). (*A*) Representative tail currents recorded at −50 mV before (Pre-drug) and after drug exposure. After drug exposure, every 10th record of the 120 peak tail currents is shown, as opposed to every record shown in the Pre-drug condition (note difference in time scale). All 120 peaks after drug exposure were fit by a single exponential ($y = Ae^{-t/\tau}$) (dashed line, Fig. 5*A*) to determine τ, the rate of development of drug blockage of HERG current. (*B*) τ, determined at multiple concentrations of dofetilide, is plotted for HERG alone (●), HERG plus KCR1 (□), and HERG plus I447V KCR1 (■). The rate of dofetilide drug blockage of HERG was reduced significantly in the presence of I447V KCR1, compared with wild-type KCR1 ($P = 0.004$, mixed ANOVA) or HERG alone. Data points represent the mean ± SEM for each concentration. The percentage of blockage of current at 20 min for 80 nM dofetilide is as follows: 95% ± 0.01, 71% ± 0.06, and 66% ± 0.05 for HERG, HERG plus wild-type KCR1, and HERG plus I447V KCR1, respectively. The number of analyzed cells is shown in parentheses next to each data point.

Discussion

We report that a *C. elegans* strain, *unc-103* (*n500*), mutant for the worm orthologue of HERG displays profound neuromuscular defects that can be used as *in vivo* screening tools for *unc-103*-modulating genes. RNAi assays demonstrate that the neuromuscular defects of *unc-103* (*n500*) are sensitive to the level of mutant channel activity. By using this strain with RNAi-based screening methods of candidate modifying genes, we present evidence that two *C. elegans* proteins, cKCR1 and MEK-14, are modulators of *unc-103* (*n500*) function *in vivo*, and thus, are potential aLQTS candidate genes.

To gain insight into the reduced-excitability phenotypes (pharyngeal pauses and impaired locomotion) associated with the UNC-103 (*n500*) A334T mutation, we constructed the analogous mutation in HERG (A653T). We found that this channel is activated at hyperpolarized potentials at which the wild-type channel is normally closed. In work from other laboratories, recordings from *C. elegans* muscle yield resting-membrane potentials ranging from −20 to −80 mV (13–15). In this voltage range, UNC-103 (*n500*) (if analogous in behavior to HERG A653T) could abnormally hyperpolarize the muscle (Fig. 3) and render the tissue less susceptible to neuronal stimulation. Alternatively, *unc-103* (*n500*) may exert its effect within the neurons that synapse onto the muscle. Unlike mammalian neurons, *C. elegans* neurons are reported to have high membrane resistance in the voltage range of −20 to −70 mV (16), implying there is little K^+ conductance at rest. Introduction of additional K^+ current via UNC-103 (*n500*) channels could, therefore, inappropriately hyperpolarize the neurons, resulting in reduced signaling to the muscle.

We assayed four different *C. elegans* genes for their ability to functionally modify UNC-103 (*n500*) *in vivo*. We chose these genes based on sequence similarity to proteins that were previ-

ously demonstrated to modify K^+ channel function in heterologous expression systems. C29F5.4 and C07D8.6 did not reveal *in vivo* modulation of *unc-103* (*n500*) in our RNAi assays. However, T24D1.4, the closest worm homologue to KCR1, which is a protein originally isolated in a screen to identify a noninactivating K^+ current from rat cerebellum (9), did modify the activity of *unc-103* (*n500*) *in vivo*. Although the function of KCR1 is not fully defined, the protein appears to be expressed in human heart and influences HERG sensitivity to drug blockage in heterologous expression systems and transfected cardiac myocytes (10). F37C12.12 (*mec-14*) has the closest amino acid similarity to *Drosophila* Hyperkinetic, and electrophysiological studies of cultured *Drosophila* giant neurons demonstrate that mutations in Hyperkinetic result in increased excitability and altered sensitivity to classical K^+ channel blockers (17). *mec-14* also modified the activity of *unc-103* (*n500*) *in vivo*. Furthermore, *mec-14* is required for normal mechanotransduction in *C. elegans* and has been proposed to act as an accessory β subunit of the degenerin channels, worm homologues to epithelial Na^+ channels (12). It is important to note that *unc-103* (*n500*) modulation by *cKCR1* and *mec-14* may not be direct. In fact, it is possible that these proteins exert their effect in noncontiguous tissue or act nonspecifically to reduce general excitability in the cells in which they are expressed. Because we are unable to coexpress these proteins with functional UNC-103 in a heterologous expression system, we do not know whether the modification occurs by means of direct or specific modulation of the UNC-103 channel, and therefore, we may conclude only that these proteins modify UNC-103 activity. *mec-14* expression is reported to occur in mechanosensory neurons (12), and Chalfie *et al*. (18) showed that ablation of AVA and AVD neurons modify pharyngeal pumping, presumably via their synapses with the RIP cells that connect pharyngeal neurons to the rest of the nervous system. Therefore, *mec-14* could be exerting its effect on UNC-103 through the same pathway. We constructed a *mec-14* (*u55*) *unc-103* (*n500*) double-mutant worm; however, as opposed to seeing a greater rescue of *unc-103* (*n500*) defects, these worms displayed additional defects. They were slower in growing and produced smaller broods than *unc-103* (*n500*) worms (data not shown). In humans, a single Kv β subunit orthologue to *mec-14* cannot be unambiguously identified. This finding influenced our decision to undertake an initial genetic screen in KCR1. We embarked on a limited genetic screen for polymorphisms in KCR1 associated with aLQTS, which revealed an association between reduced incidence of a single-nucleotide polymorphism (I447V) and untoward drug-induced QT interval prolongation. This association could suggest that I447V may play a role in protecting carriers from drug-induced cardiac arrhythmia. In support of this hypothesis, we find that coexpression of the I447V KCR1 cDNA with HERG results in a decreased rate of dofetelide blockage development, compared with either HERG alone or HERG plus wild-type KCR1.

The selective effect of *mec-14* or cKCR1 RNAi treatment on pharyngeal pumping, relative to locomotion, also underscores the importance of using multiple behavioral assays to assess UNC-103 function because particular channel functions may be context (tissue)-specific. This possibility appears to be the case with mammalian ERG as well. In the mammalian heart, ERG is involved in repolarization of the cardiac action potential, whereas in other tissues, ERG appears to have alternate functions (most notably, setting resting-membrane potentials) (19–22). We propose that the *C. elegans unc-103* (*n500*) mutant strain provides a powerful *in vivo* system for the identification of ERG-modifying proteins that could prove to be crucial modulators of HERG and proarrhythmic risk in aLQTS. Importantly, our results with candidate genes demonstrate that this system is sufficiently sensitive to allow for genome-wide screens for ERG-interacting proteins in an unbiased manner by using random mutagenesis or RNAi libraries.

We thank Poornima Madhavan and Laine Murphey for assistance with statistical analysis. We also thank David Miller, David Greenstein, and Elizabeth Link for scientific input and helpful discussions. This work was supported by National Institutes of Health Grants HL67576 (to C.I.P.), HL46681 (to J.R.B. and D.M.R.), and HL065962 (to D.M.R.).

1. Park, E. C. & Horvitz, H. R. (1986) *Genetics* **113,** 821–852.
2. Tan, H. L., Bink-Boelkens, M. T. E., Bezzina, C. R., Viswanathan, P. C., Beaufort-Krol, G. C. M., van Tintelen, P. J., van den Berg, M. P., Wilde, A. A. M. & Balser, J. R. (2001) *Nature* **409,** 1043–1047.
3. Weinshenker, D., Wei, A., Salkoff, L. & Thomas, J. H. (1999) *J. Neurosci.* **19,** 9831–9840.
4. Mitcheson, J. S., Chen, J., Lin, M., Culberson, C. & Sanguinetti, M. C. (2000) *Proc. Natl. Acad. Sci. USA* **97,** 12329–12333.
5. Timmons, L. & Fire, A. (1998) *Nature* **395,** 854.
6. Abbott, G. W., Sesti, F., Splawski, I., Buck, M. E., Lehmann, M. H., Timothy, K. W., Keating, M. T. & Goldstein, S. A. (1999) *Cell* **97,** 175–187.
7. Martens, J. R., Kwak, Y.-G. & Tamkun, M. M. (1999) *Trends Cardiovasc. Med.* **9,** 253–258.
8. Hanlon, M. R. & Wallace, B. A. (2002) *Biochemistry* **41,** 2886–2894.
9. Hoshi, N., Takahashi, H., Shahidullah, M., Yokoyama, S. & Higashida, H. (1998) *J. Biol. Chem.* **273,** 23080–23085.
10. Kupershmidt, S., Yang, I. C.-H., Hayashi, K., Wei, J., Chanthaphaychith, S., Petersen, C. I., Johns, D. C., George, A. L., Roden, D. M. & Balser, J. R. (2003) *FASEB J.*, 10.1096/fj.02–1057fje.
11. Wilson, G. F., Wang, Z., Chouinard, S. W., Griffith, L. C. & Ganetzky, B. (1998) *J. Biol. Chem.* **273,** 6389–6394.
12. Gu, G., Caldwell, G. A. & Chalfie, M. (1996) *Proc. Natl. Acad. Sci. USA* **93,** 6577–6582.
13. Davis, M. W., Somerville, D., Lee, R. Y., Lockery, S., Avery, L. & Fambrough, D. M. (1995) *J. Neurosci.* **15,** 8408–8418.
14. Franks, C. J., Pemberton, D., Vinogradova, I., Cook, A., Walker, R. J. & Holden-Dye, L. (2002) *J. Neurophysiol.* **87,** 954–961.
15. Jospin, M., Jacquemond, V., Mariol, M.-C., Segalat, L. & Allard, B. (2002) *J. Cell. Biol.* **159,** 337–348.
16. Nickell, W. T. (2002) *J. Mem. Biol.* **189,** 55–66.
17. Yao, W.-D. & Wu, C.-F. (1999) *J. Neurophysiol.* **81,** 2472–2484.
18. Chalfie, M., Sulston, J. E., White, J. G., Southgate, E., Thomson, J. N. & Brenner, S. (1985) *J. Neurosci.* **5,** 956–964.
19. Overholt, J. L., Ficker, E., Yang, T., Shams, H., Bright, G. R. & Prabhakar, N. R. (2000) *J. Neurophysiol.* **83,** 1150–1157.
20. Ohya, S., Horowitz, B. & Greenwood, I. A. (2002) *Am. J. Physiol.* **283,** C866–C877.
21. Shoeb, F., Malykhina, A. P. & Akbarali, H. I. (2003) *J. Biol. Chem.* **278,** 2503–2514.
22. Ohya, S., Asakura, K., Muraki, K., Watanabe, M. & Imaizumi, Y. (2001) *Am. J. Physiol.* **282,** G277–G287.